Renovascular anatomy as depicted by multislice helical CT

Jonathan P Hack
FCRad (D) SA
Sunninghill Hospital, Sandton

Multislice helical computed tomography (MSCT) represents state-of-the-art in modern CT imaging at present. The four channel or 'quad' multislice scanner uses between 8 and 32 detector rows for image acquisition instead of the single channel and detector row of older conventional and helical CT scanners.

A four channel (quad) multidector row CT is eight times faster than single slice CT. Eight slices are obtained per second (four slices per rotation at two rotations per second) as opposed to single slice helical CT (one slice per rotation at one rotation per second.). This provides the following benefits:

Improved temporal resolution. Faster image acquisition results in fewer motion artifacts (voluntary and involuntary).

Improved spatial resolution. Thinner slices, combined with appropriate data overlap, improves resolution along the z-axis, reducing partial volume artifacts and thus increasing diagnostic accuracy.

Improved vascular opacification. Because scanning is completed rapidly, contrast can be administered at a faster rate, improving vascular opacification and conspicuity.

Reduced image noise. Rapid scanning allows for an increase in mA thus reducing image noise and thus improving image quality.

Efficient X-ray tube utilisation. As imaging is completed more rapidly, tube heating is reduced, thus eliminating the need to wait for tube cooling between scans. During the lifetime of a tube, eight times more images are produced, reducing cost.

As shown in this pictorial essay, MSCT has an accuracy comparable to conventional angiography in identifying renal arterial anatomy and also has the added ability to simultaneously define renal venous anatomy.

Scanning technique and image display

All images were obtained during the imaging of prospective living renal donors, using an Mx8000 quad multislice CT scanner (Philips Medical Systems, Cleveland, Ohio). Post-processing was performed on an MxView workstation (Philips Medical Systems, Cleveland, Ohio).

Phase 1: 6.5 mm effective slice width images are obtained from the diaphragm to the symphasis pubis in order to evaluate for urolithiasis and to provide baseline density measurements of renal masses.

Non-ionic low osmolar contrast medium is then introduced intravenously via an antecubital vein utilising an 18 gauge cannula at a rate of 5 ml per second.

Phase 2: After a delay determined by a bolus tracking device, 1.3 mm effective slice width images are obtained from above the celiac axis to below the iliac arteries in order to map the renal arteries and veins.

Phase 3: After a delay of 65 seconds, 3.2 mm effective slice width images are obtained from the diaphragm to symphasis pubis. This allows for further evaluation of the renal venous system, the renal parenchyma and remaining intra-abdominal viscera.

Plain film post CT: This allows us to detect medullary sponge kidney, papillary necrosis, as well as duplication anomalies of the collecting systems.

Images are displayed as multiplanar reformatted images (MPR), angiographic maximum intensity projection images (MIP), 3D surface-shaded images or as 4D volume-rendered images.

Renovascular anatomy

Arterial anatomy

The renal arteries are two large arteries which arise from the sides of the aorta immediately below the superior mesenteric artery at the upper margin of L2. Their relative positions may vary according to the position of the kidneys. Although the right renal artery may travel in an oblique plane, they are often both horizontal.

In 70% of cases there are single arteries bilaterally (Figs 1 and 2).

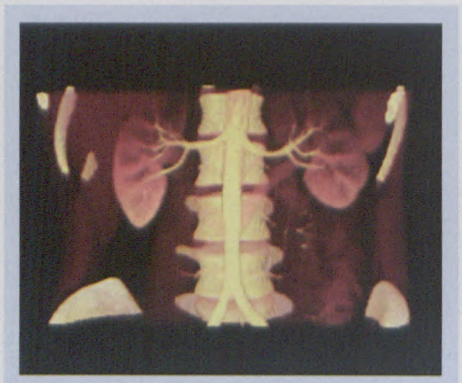

Fig.1. Volume rendered (4D) image of normal renal arteries.

Fig. 2. MIP image of normal renal arteries.

Anatomic variants

Thirty per cent of patients have multiple renal arteries, which may be : (*i*) supplementary arteries (to the hilum) (Figs 3 - 5); (*ii*) capsular arteries; (*iii*) polar arteries, which may arise from the main renal artery or from the aorta (Figs 4 - 6); and (*v*) extrahilar branching (Figs 3 and 4).

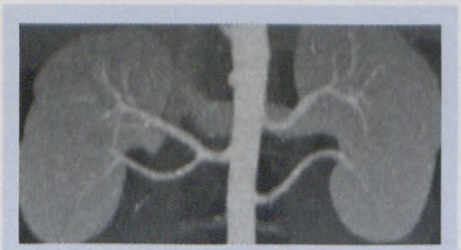

Fig. 3. MIP image demonstrating a supplementary artery on the left and early extra hilar branching on the right.

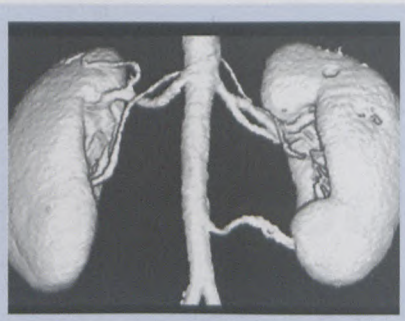

Fig. 4. 3D surface shaded image demonstrating bilateral supplementary arteries, early extra hilar branching on the left and a left sided polar artery.

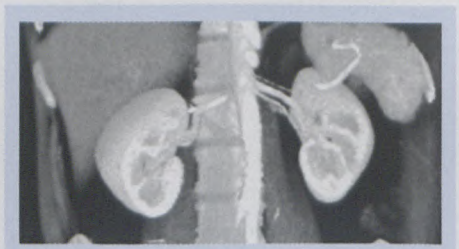

Fig. 5. 4D volume rendered image demonstrating a left sided polar and supplementary artery.

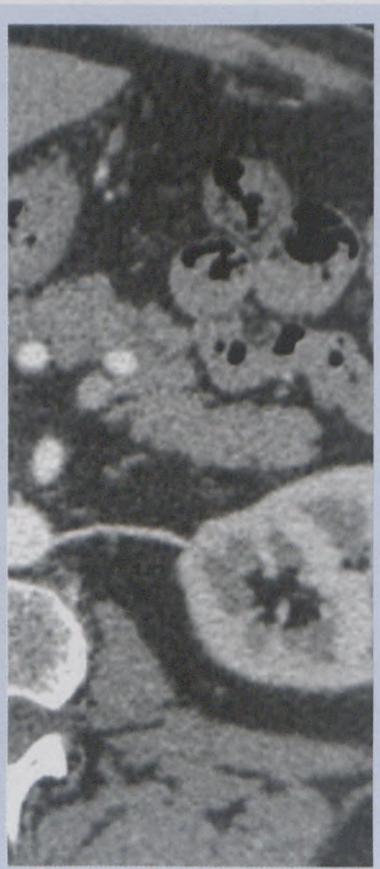

Fig. 6. Curved MPR demonstrating a small left sided polar artery.

Venous anatomy

The right renal vein is short (± 2 - 2.5 cm) and is single in 85% of cases. It does not usually receive any significant tributaries.

The left renal vein is long (± 8.5 cm). It is single and preaortic in position in 85% of cases and it receives the left spermatic, inferior phrenic and, usually, the left adrenal veins (Figs 7 and 8). It passes just below the origin of the superior mesenteric artery.

Fig. 7. Curved MPR demonstrating normal renal veins.

Fig. 8. Curved MPR demonstrating large left gonadal veins and the left adrenal vein.

Anatomic variants

Right renal vein: (*i*) multiple veins (Fig 9); and (*ii*) gonadal and adrenal veins may occasionally drain into the right renal vein.

Left renal vein: (*i*) multiple veins (Fig. 10); (*ii*) circumaortic vein (Figs 11 and 12); and (*iii*) retro- aortic vein (Fig. 13).

Lumbar veins may drain into the renal vein (Fig. 14).

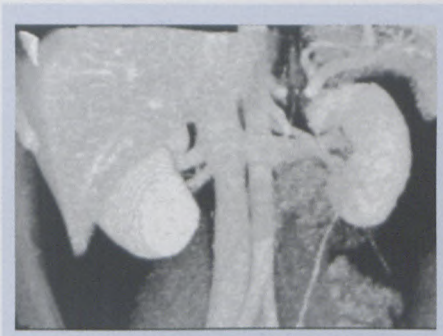

Fig. 9. Volume rendered image demonstrating complete duplication of the right renal vein.

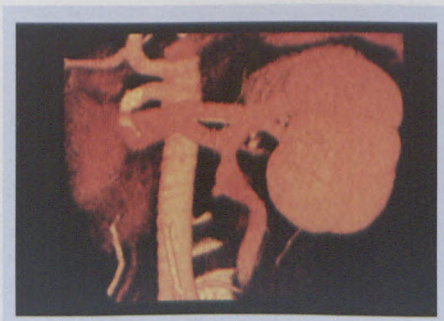

Fig. 10. Volume rendered image demonstrating partial duplication of the left renal vein and a large left gonadal vein.

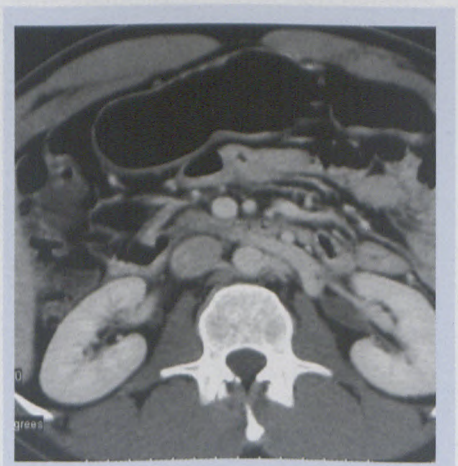

Fig. 11. Curved MPR demonstrating a circumaortic left renal vein.

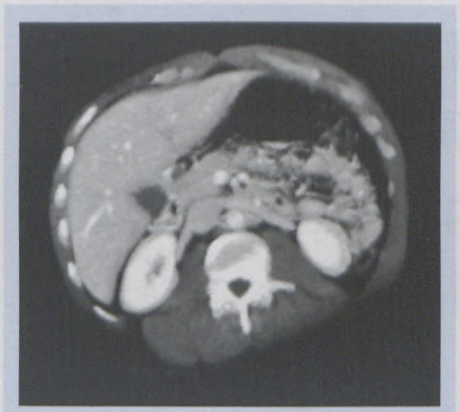

Fig. 12. Volume rendered image demonstrating a circumaortic left renal vein.

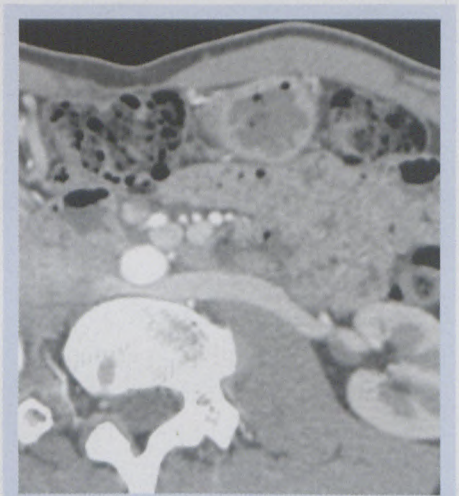

Fig. 13. Curved MPR demonstrating a retro-aortic left renal vein.

Fig. 14. Curved sagittal MPR demonstrating a large lumbar vein draining into the left renal vein.

Acknowledgement

Images 3, 4 and 10 courtesy of J Rydberg, *et al.*

Further reading

1. Pozniac MA, Balison DJ, Lee FT Jr, Tambeaux RH, Uehling DT, Moon TD. CT angiography of potential renal transplant donors. *Radiographics* 1998; **18:** 556-587.
2. Rydberg J, Kopecky KK, Tann M, *et al.* Evaluation of prospective living renal donors for laparoscopic nephrectomy with multislice CT: The marriage of minimally invasive imaging with minimally invasive surgery. *Radiographics* 2001; **21:** S223-S226.
3. Gray G. *Gray's Anatomy.* The Classic Collector's Edition. New York: Bounty Books, 1977: 556-557, 619.
4. http://www.indyrad.iupui.edu/multislice-ct/ (last accessed 01 April 2003).